RSC Advances

Cite this: *RSC Advances*, 2012, **2**, 5094–5097

www.rsc.org/advances

COMMUNICATION

NO*x* storage and reduction with methane by plasma at ambient temperature†

Hui Wang, Qinqin Yu, Tong Liu, Liping Xiao and Xiaoming Zheng*

Received 19th January 2012, Accepted 3rd April 2012
DOI: 10.1039/c2ra20115a

NO*x* storage and reduction with CH_4 by a plasma process was proposed for NO*x* removal at ambient temperature. The efficiency of this new process for NO*x* removal could achieve 95% at ambient temperature. NO*x* removal *via* cyclic operation has also been investigated, maintaining efficieniency above 90%.

In the light of stringent world-wide environmental legislation, nitrogen oxide NO*x* (NO, NO_2, N_2O), one of the most dangerous gaseous pollutants, requires new abatement technologies.[1] Selective catalytic reduction using methane as a reducing agent (CH_4-SCR) has been studied as a desirable technology for removal of NO*x* in the presence of excess oxygen for a long time.[2] CH_4 has attracted considerable attention because of its vast reserves, low cost and easy handling. However, it is difficult to activate CH_4 for the high stability of the C–H bonds. To reduce the reaction activation energy through catalysis is one of the main challenges in CH_4–SCR. Unfortunately, the existing catalysts, even modified by noble metal such as Pd/Co/mordenite,[3] Pt/Co/mordenite[4] and Pt/Co/ZSM-5,[5] exhibited satisfactory activity for CH_4–SCR only when the temperature was more than 673 K. High reaction temperature means high energy consumption, which is unacceptable considering industrial applications, especially for stationary sources. It is hence meaningful to find a solution that can improve the low-temperature activity of the CH_4–SCR.

Non-thermal plasma (NTP) could activate molecules including NO*x* and hydrocarbons at ambient temperature. Thus, there has been extensive research on NTP for NO*x* removal recently. Plasma procedures for NO*x* removal mainly include plasma-assisted SCR[6] and plasma-derived NO decomposition process.[7] Nonetheless, it requires high energy-consumption to remove NO*x* at low concentration from exhaust gas or flue gas by constant plasma discharge. To solve the problem, an improved plasma process was proposed by several groups.[8] The pollutant is first enriched on the adsorbents, and then the adsorbed pollutant is desorbed or decomposed by plasma in a short time. But an effective de-NO*x* by plasma is barely possible in the absence of an oxygen atmosphere.[9] O_2 derived from carrier gas (air or combustion gas) and NO*x* decomposed can react with N_2 to generate a considerable amount of NO*x* in plasma. Briefly, the reverse reaction of NO*x* decomposition leads to a reduction of the total de-NO*x* efficiency.

Deriving from the traditional NO*x* storage and reduction (NSR) technology[10] combined NTP, we reported herein a NSR process in plasma using CH_4 as a reducing agent. First, diluted NO*x* was on using commercial H-ZSM-5 (Si/Al ratio at 22, without further modification) for a long time. Then, the adsorbed pollutant was reduced with CH_4 by NTP in a few minutes. Notably, in the discharge stage, we chose combustion gas (oxygen-deficient gas containing nearly 5% O_2) instead of air as a carrier gas. Moreover, the whole cyclic process carried out at ambient temperature. Finally, a high-efficient process for NO*x* removal was obtained at low energy consumption, even without the use of any noble metal.

Fig. 1 shows the schematic diagram of the combined CH_4-NSR and plasma system. The dielectric barrier discharge (DBD) reactor consists of a quartz tube (i.d. 8.5 mm) as the reactor as well as the dielectric barrier, a stainless steel rod (o.d. 3.5 mm) as the high-voltage electrode, and a stainless steel wire mesh wrapped on the outside of the quartz tube as the grounding electrode. H-ZSM-5 was filled in the discharge gap between the high-voltage electrode and the quartz tube. The DBD reactor was energized by an AC power source (Nanjing Suman Electronics Co. Ltd). The waveforms of the discharge current and the applied voltage were monitored with a digital oscilloscope (Tektronix, TDS 1002B-SC). Discharge power was measured by the V–Q Lissajous program.

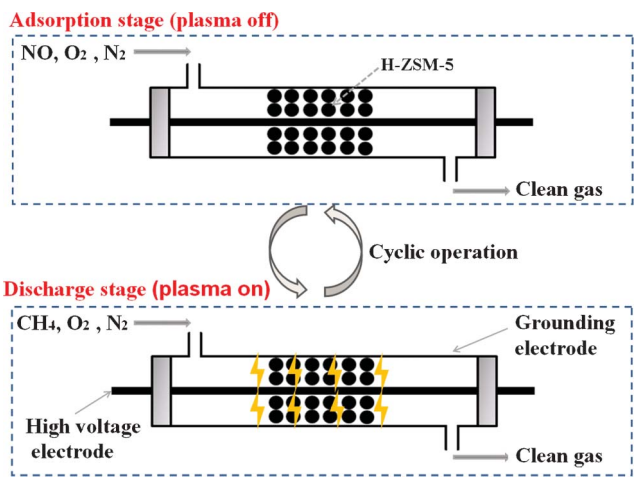

Fig. 1 Schematic diagram of the combined CH_4–NSR and plasma system.

Key Lab of Applied Chemistry of Zhejiang Province, Zhejiang University, Hangzhou, 310028, China. E-mail: xmzheng@zju.edu.cn; Fax: (+)86 571 88273283; Tel: (+)86 571 88273417

† Electronic Supplementary Information (ESI) available. See DOI: 10.1039/c2ra20115a/

Fig. 2 (a) shows the conversion of the adsorbed NO*x* to N_2 on H-ZSM-5 in CH_4–NSR by plasma as a function of discharge power. H-ZSM-5 acted as an adsorbent for NO*x* at the first stage and a catalyst at the second stage owing to its acid site. Clearly, the conversion of adsorbed NO*x* to N_2 improved greatly with increasing discharge power, reaching 95% at 6.7 W. High energy density is beneficial to NO*x* conversion in CH_4–NSR, according with the results reported in other reaction systems.[11] Moreover, CH_4 conversion remains 100% at different discharge power during the reaction as shown in Fig. 2 (b). And the selectivity of CH_4 to CO_2 was also nearly 100%, because CO was easily oxidized to CO_2 in plasma. At the same time, no NO*x* was detected on the adsorbent at each discharge power after the discharge stage through a temperature-programmed desorption (TPD) process. Fig. 2 (c) shows that NO*x* conversions in NO*x* decomposition without CH_4 are all below 40% due to the reverse reaction of NO*x* decomposition (NO*x* formation reaction). Obviously, CH_4 enhanced the total NO*x* conversion. On one hand, a suitable amount of CH_4 could play a role as a reducing agent in NSR; on the other hand, CH_4 oxidation consumed O_2 to restrain the reverse reaction of NO*x* decomposition effectively. On-line mass spectrometry (MS) detected no N_2O_5, N_2O_4, or N_2O_3 produced during the reaction. Quantitative analysis indicated that the selectivity of NO*x* to N_2O was lower than 0.5% in CH_4-NSR.

The direct decomposition of NO (gaseous phase) in plasma has been investigated. Herein, through NO decomposition, we deduced fundamental rules and phenomenon about NO abatement (decomposition or reduction) in plasma. The result is shown in Fig. 3 (A). As the discharge power increased, the decomposition of 50 000 ppm NO at high flow rate (80 mL min^{-1}) moved up significantly, achieving more than 99% at 6.72 W. This phenomenon suggested that high energy density led to high NO*x* conversion once again. When the total flow rate decreased to 30 mL min^{-1} to enhance the energy density of system, NO decomposed to N_2 almost 100% at all discharge power except for the lowest, 3 W. Reducing NO concentration (2000 ppm or 10 000 ppm) in the feed to make

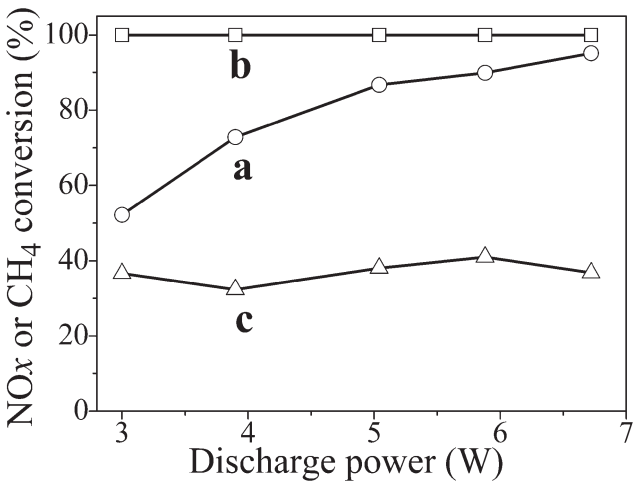

Fig. 2 (a) Conversion of adsorbed NO*x* to N_2 and (b) CH_4 to CO_2 in CH_4-NSR and (c) conversion of adsorbed NO*x* in decomposition of NO*x* without CH_4 as a function of discharge power. *Conditions*: 1 g H-ZSM-5, 30 mL min^{-1} flow rate of oxygen-deficient air (5% O_2 + 95% N_2) with or without 1.67% CH_4, total input energy of the plasma ($P \times t_{discharge}$) is fixed at 0.896 W h.

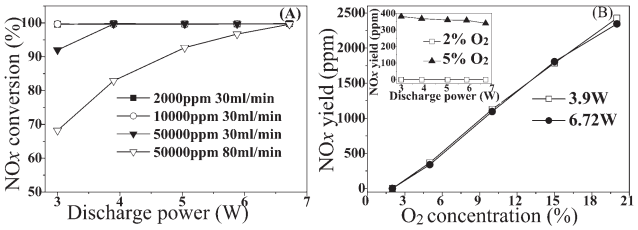

Fig. 3 (A) NO decomposition in plasma as a function of discharge power. (B) NO*x* yield in the reaction of O_2 with N_2 as a function of O_2 concentration and discharge power (inset) in plasma. *Conditions A*: various concentration NO (balanced N_2) with a certain flow rate in the absence of adsorbent. *Conditions B*: 30 mL min^{-1} of total flow rate, discharge power is 6.72 W in the absence of adsorbent.

further improvement of energy density, the decomposition of NO was 100% even at 3 W. Fig. 3 (B) displays the effect of O_2 concentration and discharge power on the reverse reaction of NO*x* decomposition (NO*x* formation reaction). The yield of NO*x* increased rapidly with increasing the O_2 concentration. Interestingly, the discharge power did not affect the yield of NO*x*, suggesting that energy density did not affect the reverse reaction of NO*x* decomposition. Based on the above analysis, the phenomenon shown in Fig. 2 could be explained. In order to improve the NO*x* conversion, O_2 concentration in the system must be controlled by introducing of CH_4 in the feed. Enhancing discharge power to raise the energy density of system was beneficial for NO*x* removal and did not affect the corresponding reverse reaction.

In order to further optimize the discharge process, we investigated the effect of flow rate and CH_4/O_2 molar ratio on the conversion of adsorbed NO*x* to N_2 in the discharge stage. Fig. 4 (a) shows that NO*x* conversion decreased with increased flow rate. When the flow rate increased, the energy density of the system decreased at the same discharge power. Low energy density led to low NO*x* conversion, in agreement with the result from Fig. 2 (a). Actually, the demand for lower flow rate at the discharge stage will never be a drawback to this

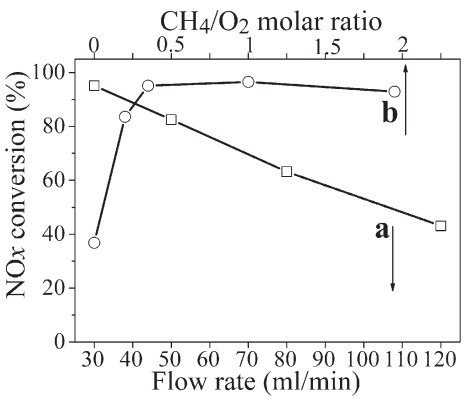

Fig. 4 Effect of (a) flow rate and (b) CH_4/O_2 molar ratio on the conversion of adsorbed NO*x* in CH_4-NSR. *Conditions a*: 1 g H-ZSM-5, different flow rate of oxygen-deficient air (5% O_2 + 95% N_2) with 1.67% CH_4, total input energy of the plasma is fixed at 6.72 W × 8 min. *Conditions b*: 1 g H-ZSM-5, 30 mL min^{-1} flow rate of oxygen-deficient air (5% O_2 + 95% N_2) with various CH_4/O_2 molar ratios, total input energy of the plasma is fixed at 6.72 W × 8 min.

proposed technology, because the discharge time is very short. In addition, low flow rate can cut down the consumption of the reducing agent CH_4 for NSR. On the other hand, the adsorption stage, for reaction long times, is not affected by high flow rate due to the superior storage performance of H-ZSM-5 for NO*x*. Fig. 4 (b) displays NO*x* conversion as a function of CH_4/O_2 molar ratio. The positive effect of CH_4 added in the feed was remarkable. The conversion of NO*x* to N_2 was significantly higher (more than 95%) when the CH_4/O_2 molar ratio was between 0.333 and 1. When the CH_4/O_2 molar ratio exceeded 1, the NO*x* conversion fell off and an excess of CH_4 also could bring into the greenhouse effect.

Cyclic operation of the present process for NO*x* removal has been investigated (Fig. 5). Notably, between the intermissions of two cycles, the absorbent H-ZSM-5 does not need to be treated for regeneration in any way. Over the adsorption stage, a large amount of NO*x* could be completely trapped on H-ZSM-5, due to no NO*x* remaining on the adsorbent after the discharge stage. In the discharge stage, the conversion of adsorbed NO*x* to N_2 decreased a little in the second time, and then kept at above 90% in continuing reaction cycles. NO*x* removal of cyclic operation was satisfactory. XRD patterns of H-ZSM-5 before and after reaction (Fig. 1S in the ESI†) showed that H-ZSM-5 still kept its crystalline structure during the cyclic reaction. Both results suggested that the performance of H-ZSM-5 is stable under the process conditions.

In conclusion, the CH_4-NSR process by plasma could remove NO*x* efficiently achieving 95%removal at ambient temperature. Plasma primarily activated the gaseous molecule. CH_4 introduced into the system played an important role as a reducing agent and also restrained the reverse reaction of NO*x* decomposition effectively. A high energy efficiency for the removal of NO*x* was obtained, 0.416 mmol NO*x*/W h (ESI†), due to the long-time adsorption and short-time discharge in the process. The energy efficiency of the new process proposed was improved, compared with the conventional thermal catalytic process. Thus, we believe that this new de-NO*x* technology has broad application prospects.

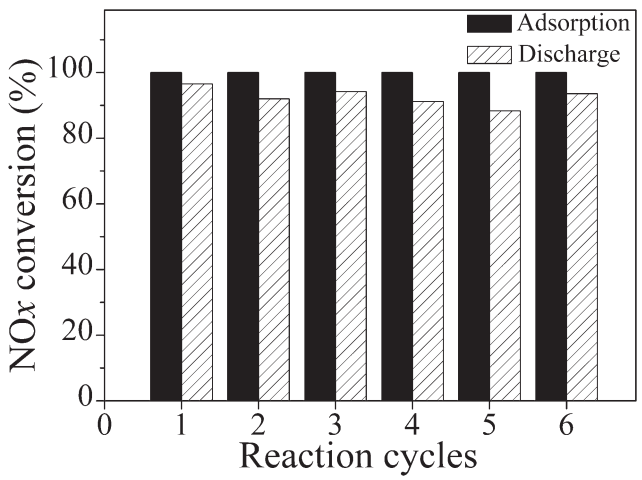

Fig. 5 Cyclic operation of the present adsorption–discharge process for NO*x* removal: percentage of NO*x* abatement in the adsorption stage (black) and conversion of adsorbed NO*x* to N_2 in the discharge stage (slash). *Conditions*: in the adsorption stage, 1 g H-ZSM-5 adsorbed 66 mL min^{-1} flow rate containing 1840 ppm NO (8% O_2, balanced N_2) for 1 h; in the discharge stage, 30 mL min^{-1} flow rate of oxygen-deficient air (5% O_2 + 95% N_2) with 5% CH_4, total input energy of the plasma is fixed at 6.72 W × 7 min = 0.784 W h.

Experimental section

Before the experiment, 1 g H-ZSM-5 (Si/Al = 22) (20–40 mesh) was pretreated at 773 K for 60 min in N_2 flow, and then cooled down to room temperature. The whole experiment consisted of two stages. In the adsorption stage (plasma off), a flowing mixed gas containing 1840 ppm NO and 8% O_2 balanced N_2 was introduced into the catalyst-packed dielectric barrier discharge (DBD) reactor at a total flow rate of 66 mL min^{-1}. This stage lasted for 1 h at 308 K and H-ZSM-5 absorbed 0.326 mmol NO*x*. In the discharge stage (plasma on), the gas stream oxygen-deficient air (5% O_2 + 95%N_2) and a small quantity of CH_4 was switched into the DBD reactor. This discharge process just lasted several minutes at room temperature. The total input energy of the plasma ($P \times t_{discharge}$) is fixed at 0.896 W h (except the cyclic experiment).

The concentrations of NO and NO_2 were analyzed online by a chemiluminescent NO/NO_2/NO*x* analyzer (Eco Physics). N_2O was analyzed using a Fuli-9750 gas chromatograph (GC) with TCD and a Porapak Q column. The definitions of the conversion of NO*x* to N_2 and energy efficiency were defined as follows:

$$\mathrm{Conv.NO}x \rightarrow \mathrm{N_2}(\%) = \frac{n_{NOx}^{absorbed} - n_{NOx}^{emitted} - n_{NOx}^{residual}}{n_{NOx}^{absorbed}} \times 100\%$$

$$\text{energy efficiency}(\mathrm{mmol/W \cdot h}) = \frac{n_{NOx}^{absorbed} \times \mathrm{Conv.}_{NOx \rightarrow N_2}}{P \times t_{discharge}}$$

where $n_{NOx}^{absorbed}$ is the amount of NO*x* adsorbed on H-ZSM-5 at the adsorption stage; $n_{NOx}^{emitted}$ is the amount of NO*x* (NO, NO_2, N_2O) emitted to the exhaust during the plasma stage; $n_{NOx}^{residual}$ is the amount of NO*x* species remaining on the catalyst after the plasma stage, which was determined by a temperature-programmed desorption (TPD) process; P is the discharge power (W); $t_{discharge}$ is the discharge time in the discharge stage.

Acknowledgements

This work is financially supported by Major project of Zhejiang Province (No.2009C11141), the National Natural Science Foundation of China (No.20977080) and the Natural Science Foundation of Zhejiang Province (No.J20091504).

References

1 (*a*) P. Forzatti, I. Nova and E. Tronconi, *Angew. Chem.*, 2009, **121**, 8516; (*b*) C. Petitto, H. P. Mutin and G. Delahay, *Chem. Commun.*, 2011, **47**, 10728.
2 (*a*) M. C. Campa, S. De Rossi, G. Ferraris and V. Indovina, *Appl. Catal., B*, 1996, **8**, 315; (*b*) L. Gutierrez and E. A. Lombardo, *Appl. Catal. A*, 2009, **306**, 107.
3 (*a*) F. Bustamante, F. Córdoba, M. Yates and C. M. de Correa, *Appl. Catal., A*, 2002, **234**, 127; (*b*) L. F. Córdoba, G. A. Fuentes and C. M. de Correa, *Microporous Mesoporous Mater.*, 2005, **77**, 193.
4 (*a*) L. Gutierrez, A. V. Boix, E. A. Lombardo and J. L. G. Fierro, *J. Catal.*, 2001, **199**, 60; (*b*) L. Gutierrez, M. A. Ulla, E. A. Lombardo, A. Kovacs, F. Lonyi and J. Valyon, *Appl. Catal., A*, 2005, **292**, 154.
5 L. Gutierrez, A. Boix and J. O. Petunchi, *J. Catal.*, 1998, **179**, 179.
6 (*a*) D. N. Tran, C. L. Aardahl, K. G. Rappe, P. W. Park and C. L. Boyer, *Appl. Catal., B*, 2004, **48**, 155; (*b*) J. L. Hueso, J. Cotrino, A. Caballero, J. P. Espinós and A. R. González-Elipe, *J. Catal.*, 2007, **247**, 288.

7 (*a*) J. Luo, S. L. Suib, M. Marquez, Y. Hayashi and H. Matsumoto, *J. Phys. Chem. A*, 1998, **102**, 7954; (*b*) S. L. Suib, S. L. Brock, M. Marquez, J. Luo, H. Matsumoto and Y. Hayashi, *J. Phys. Chem. B*, 1998, **102**, 9661.
8 (*a*) M. Okubo, G. Tanioka, T. Kuroki and T. Yamamoto, *IEEE Trans. Ind. Appl.*, 2002, **38**, 1196; (*b*) H. H. Kim, A. Ogata and S. Futamura, *Appl. Catal., B*, 2008, **79**, 356; (*c*) Q. Q. Yu, H. Wang, T. Liu, L. P. Xiao, X. Y. Jiang and X. M. Zheng, *Environ. Sci. Technol.*, 2012, **46**, 2337.
9 M. Baeva, H. Gier, A. Pott, J. Uhlenbusch, J. Hoschele and J. Steinwandel, *Plasma Sources Sci. Technol.*, 2002, **11**, 1.
10 (*a*) L. Castoldi, I. Nova, L. Lietti and P. Forzatti, *Catal. Today*, 2004, **96**, 43; (*b*) S. Roy and A. Baiker, *Chem. Rev.*, 2009, **109**, 4054.
11 (*a*) A. Ogata, H. Einaga, H. Kabashima, S. Futamura, S. Kushiyama and H. H. Kim, *Appl. Catal., B*, 2003, **46**, 87; (*b*) A. M. Harling, D. J. Glover, J. C. Whitehead and K. Zhang, *Ind. Eng. Chem. Res.*, 2008, **47**, 5856.